



HAL
open science

Late Quaternary micromammals and the precipitation history of the southern Cape, South Africa

J. Tyler Faith, Brian M. Chase, D. Margaret Avery

► **To cite this version:**

J. Tyler Faith, Brian M. Chase, D. Margaret Avery. Late Quaternary micromammals and the precipitation history of the southern Cape, South Africa. *Quaternary Research*, 2019, 91 (2), pp.848-860. 10.1017/qua.2018.105 . hal-02123506

HAL Id: hal-02123506

<https://hal.science/hal-02123506>

Submitted on 12 Jul 2022

HAL is a multi-disciplinary open access archive for the deposit and dissemination of scientific research documents, whether they are published or not. The documents may come from teaching and research institutions in France or abroad, or from public or private research centers.

L'archive ouverte pluridisciplinaire **HAL**, est destinée au dépôt et à la diffusion de documents scientifiques de niveau recherche, publiés ou non, émanant des établissements d'enseignement et de recherche français ou étrangers, des laboratoires publics ou privés.

1 **Late Quaternary micromammals and the precipitation history of the**
2 **southern Cape, South Africa**

3
4 **The authors do not recommend the distribution of this version**
5 **of this article.**

6 **The article is freely available upon request.**

7 **To receive a copy, please send a request to Brian Chase at:**

8 **brian.chase@umontpellier.fr**

9
10
11
12 **J. Tyler Faith**

13 Natural History Museum of Utah & Department of Anthropology
14 University of Utah
15 Salt Lake City, UT 84108 USA
16 E-mail: jfaith@nhmu.utah.edu; Telephone: (801) 581-8572

17
18 **Brian M. Chase**

19 Centre National de la Recherche Scientifique
20 Institut des Sciences de l'Evolution de Montpellier
21 Université Montpellier
22 34095 Montpellier, France
23 E-mail: brian.chase@univ-montp2.fr

24
25 **D. Margaret Avery**

26 Iziko South African Museum
27 P.O. Box 61
28 Cape Town, 8000 South Africa
29 E-mail: mavery@iziko.org.za

30
31 Manuscript draft: June 7, 2018

32 **ABSTRACT**

33 The southern Cape of South Africa is important to understanding regional climate
34 because it straddles the transition between the winter and summer rainfall zones. We
35 examine late Quaternary changes in rainfall seasonality and aridity through analysis of
36 micromammal assemblages from three sites: Boomplaas Cave and Nelson Bay Cave in
37 the aseasonal rainfall zone, and Byneskranskop 1 in the winter rainfall zone. Our
38 interpretation is based on analysis of 123 modern micromammal assemblages
39 accumulated by barn owls (*Tyto alba*), which empirically links species composition to
40 climate. The Pleistocene record (~65 to 12 ka) from Boomplaas Cave, together with the
41 Last Glacial Maximum (LGM) samples from Nelson Bay Cave, indicates enhanced
42 winter rainfall, especially during the LGM. Boomplaas Cave documents progressive
43 aridification from the LGM to the earliest Holocene, followed by a return to moderately
44 humid conditions through the Holocene.. Byneskranskop 1 indicates a dominance of
45 winter rains over the last 17 ka, and a shift from an arid middle Holocene to a humid
46 later Holocene. Agreement between the micromammal record and other local and
47 regional proxies reinforces the potential of southern African micromammal assemblages
48 as paleoclimate indicators.

49

50 **Keywords:** Aridity, Holocene, Last Glacial Maximum, Mammals, Paleoclimate,

51 Precipitation, Seasonality

52 INTRODUCTION

53 The southern Cape of South Africa, here defined as the region encompassing the
54 southern coastal plains and the east-west trending ranges of the Cape Fold Belt,
55 straddles the transition between the winter rainfall zone (WRZ; > 66% of mean annual
56 precipitation falls from April to September) to the west and the summer rainfall zone
57 (SRZ; >66% of mean annual precipitation falls from October to March) to the east
58 (sensu Chase and Meadows, 2007; Fig. 1). The WRZ receives most of its rainfall from
59 the frontal systems associated with the westerly storm track, which migrates northward
60 during the austral winter. In contrast, precipitation in the SRZ is related to tropical
61 easterly flow, which advects moisture from the Indian Ocean during the summer months
62 (Tyson, 1986; Chase and Meadows, 2007). Because most of the southern Cape falls
63 within the aseasonal rainfall zone (ARZ; Fig. 1), receiving precipitation throughout the
64 year from both sources and their combined effects (Chase et al., 2017, 2018), the
65 region is uniquely positioned to inform on the history of these temperate and tropical
66 circulation systems.

67 Quaternary variability in these two systems in southern Africa has been a focus
68 of research for decades (van Zinderen Bakker, 1967, 1976; Heine, 1982; Cockcroft et
69 al., 1987; Deacon and Lancaster, 1988). The dominant paradigm suggests that the
70 boundaries of the WRZ and SRZ have shifted through time, due to the enhancement of
71 winter rainfall during glacials and enhancement of summer rainfall during interglacials
72 (see reviews in Deacon and Lancaster, 1988; Partridge et al., 1990; Chase and
73 Meadows, 2007; Chase et al., 2017). However, the precipitation history of the southern
74 Cape remains unclear and debated. For instance, cool phases of the Pleistocene have

75 been associated with enhanced winter rains (Faith, 2013b; Sealy et al., 2016; Chase et
76 al., 2018), whereas some records link cool conditions to intensified summer rains (Bar-
77 Matthews et al., 2010). Even the most basic particulars—were glacials wetter or drier
78 than interglacials?—are uncertain (Chase and Meadows, 2007; Marean et al., 2014),
79 with some, for example, characterizing the Last Glacial Maximum (LGM: 26.5-19 ka;
80 Clark et al., 2009) as harsh and arid (e.g., Avery, 1982; Deacon et al., 1984; Deacon
81 and Lancaster, 1988) or humid and highly productive (e.g., Faith, 2013b; Chase et al.,
82 2017, 2018). Uncertainty in these and other aspects of the region’s precipitation history
83 stems in part from a lack of records that inform directly on the relevant climate
84 parameters (Chase et al., 2013). This is exacerbated by a combination of seemingly
85 contradictory lines of evidence (e.g., Avery, 1982, 2004), conflicting interpretations of
86 the evidence (e.g., Deacon et al., 1984; Faith, 2013a), and a substantial degree of not
87 yet well-understood spatial variation (Chase et al., 2015b; Chase et al., 2017), such as
88 evidence indicating that coastal archives are out of phase with those found in the
89 interior (Chase and Quick, 2018).

90 Of the various proxy records from the southern Cape (reviewed in Chase and
91 Meadows, 2007; Marean et al., 2014), the fossil record of raptor-accumulated
92 micromammal assemblages from cave deposits features prominently in discussion of
93 past climate and environment (e.g., Avery, 1982, 1983; Deacon et al., 1984; Avery,
94 1987; Thackeray, 1987; Avery, 1990; Thackeray, 1990; Avery, 1993, 2004; Matthews et
95 al., 2011; Nel and Henshilwood, 2016; Nel et al., 2018; Thackeray and Fitchett, 2016).
96 Such assemblages are widely used to inform on climate in a diverse range of
97 geographic and temporal settings (e.g., Andrews, 1990), though interpretations of those

98 from the southern Cape are, like other records from the region, not always in agreement
99 (e.g., Avery, 1982; Thackeray, 1987; Avery, 2004; Faith, 2013a). Our aim here is to
100 revisit several key late Quaternary micromammal sequences, with a focus on their
101 implications for the region's precipitation history. The main contribution of this study is
102 that our interpretations are informed by a large sample of modern micromammal
103 assemblages from southern Africa. We use these assemblages to relate variation in
104 taxonomic composition to variation in climate, which provides an empirical framework
105 for interpreting taxonomic fluctuations in the past.

106

107 **MATERIALS AND METHODS**

108 **Micromammal assemblages**

109 Our analysis makes use of taxonomic abundance data—quantified according to the
110 minimum number of individuals (MNI) after Avery (1982)—from modern and fossil
111 micromammal assemblages. The species included in our analysis typically weigh less
112 than 150 grams and include rodents (Rodentia), shrews (Soricidae), elephant shrews
113 (Macroscelididae), and golden moles (Chrysochloridae). The taxonomy used here
114 follows Wilson and Reeder (2005). Bats are not considered in our analysis.

115 The modern sample includes 123 assemblages collected by D.M.A. from barn
116 owl (*Tyto alba*) roosts across southern Africa (Fig. 1) (see Avery, 1999), and currently
117 curated at the Iziko South African Museum in Cape Town (Supplementary Tables 1-2).
118 At each sample locality, whole or partial barn-owl pellets were collected and, where
119 appropriate, bulk debris from collapsed pellets was bagged for subsequent analysis.
120 Some assemblages, such as those from West Coast National Park (Avery, 1992), were

121 sampled multiple times. Assemblage sample size ranges from 24 to 6943 individuals
122 (median = 243.5). Important to our work here, these assemblages encompass a broad
123 range of precipitation regimes (from 19-91% summer rain), occurring in the SRZ (n =
124 60), the WRZ (n = 41), and in the ARZ (n = 22). Following the UNEP (United Nations
125 Environment Programme) (1997) classification scheme for aridity, sites are
126 characterized by climates that are arid (n = 41), semi-arid (n = 52), dry sub-humid (n =
127 28), and humid (n = 2) (Fig. 2). We caution that the small sample of assemblages from
128 humid climates limits our ability to model the relationship between species composition
129 and climate at the more humid end of the spectrum.

130 Fossil data are derived from Avery (1982) and include the late Quaternary
131 assemblages from three southern Cape archaeological sites: Boomplaas Cave
132 (Deacon, 1979) and Nelson Bay Cave in the ARZ (Klein, 1972; Deacon, 1984) and
133 Byneskranskop 1 (Schweitzer and Wilson, 1982) in the WRZ (Fig. 1). These sites were
134 selected to the exclusion of a few others from the region (e.g., Die Kelders and Klasies
135 River) because of their more robust chronologies (Loftus et al., 2016; Pargeter et al.,
136 2018), and because they include deposits sampling the transition from glacial to
137 interglacial conditions. Located on the southern flanks of the Swartberg range ~80
138 km inland, Boomplaas Cave was excavated by Hilary Deacon in the 1970s (Deacon,
139 1979; Deacon, 1984). It provides the longest sequence examined here, spanning the
140 last ~65 ka, with a particularly well-dated sequence after the onset of the LGM (Pargeter
141 et al., 2018). Nelson Bay Cave is located on the Robberg Peninsula on the southern
142 Cape coastline. It was excavated by Ray Inskeep (1987) and later by Richard Klein
143 (1972; see also Deacon, 1984). Microfauna data are only available from layers YSL and

144 YGL (Klein's excavation), dating to 23.5-21.0 ka and 22.1-16.3 ka, respectively (Loftus
145 et al., 2016). Lastly, Byneskranskop 1 is located at the western margin of the southern
146 Cape, ~7 km from the modern coastline. Excavations by Franz Schweitzer in the 1970s
147 (Schweitzer and Wilson, 1982) uncovered a stratified sequence spanning the last 17 ka
148 (Loftus et al., 2016). The stratigraphy, chronology, and taxonomic abundance data for
149 each of the assemblages examined here are reported in Supplementary Table 3.

150 Details concerning the taphonomic histories of the fossil assemblages require
151 that we make a few assumptions. First, we note that the microfauna from Boomplaas
152 Cave were recovered using a combination of 2- and 3-mm mesh, whereas 3-mm mesh
153 was used for the other two sites. Because finer mesh was not used at any site, there is
154 potential for taphonomic bias against recovery of smaller specimens and smaller-bodied
155 species (e.g., Lyman, 2012). We assume that the effects of such bias are consistent
156 within a given site. In addition, we must also make an assumption about the
157 accumulator(s) of the micromammal remains. Avery (1982) argued that barn owls were
158 the primary accumulators of the microfauna from all three sites. This inference was
159 based on assessment of the ecology of potential accumulators and the represented
160 prey species, as her analysis was conducted before development of taphonomic
161 approaches for identifying the likely bone accumulators (e.g., Andrews, 1990). However,
162 there is reason to believe that other raptor species could have accumulated some of the
163 microfaunal remains examined here. For example, taphonomic analysis of the
164 macrofauna from Boomplaas Cave indicates that some of the smaller species (e.g.,
165 leporids, hyraxes, smaller ungulates) were accumulated by very large raptors (Faith,
166 2013a). Likewise, spotted eagle owls (*Bubo africanus*) are implicated in the taphonomic

167 histories of other microfaunal assemblages from the region (Matthews et al., 2011; Nel
168 et al., 2018), though they generate microfaunal assemblages that are very similar in
169 composition to those of barn owls (Reed, 2005). In the absence of taphonomic analysis
170 of the micromammal assemblages, we assume that contributions by other bone
171 accumulators have not overprinted the environmental signal in a manner that would
172 substantially alter our results.

173 Barn owl assemblages are usually thought to provide a reasonably accurate
174 representation of the local micromammal community (e.g., Andrews, 1990; Fernández-
175 Jalvo et al., 2016). They typically forage within a radius of up to 2-3 km (Andrews,
176 1990), preferentially targeting open habitats where it is easier to locate and capture prey
177 (Taylor, 1994). The relatively small foraging radius implies that the modern and fossil
178 assemblages examined here provide highly localized samples of the micromammal
179 community. It follows that they may be especially sensitive to local environmental
180 conditions. This spatial scale must be considered when interpreting micromammal
181 assemblages in terms of much larger-scale climate phenomena (see Discussion). The
182 open-habitat bias is less of a concern here, as it is likely to be consistent across all
183 assemblages.

184

185 **Analytical methods**

186 For each of the 123 modern micromammal assemblages, we extracted data on rainfall
187 seasonality and aridity from the WorldClim global climate database (Hijmans et al.,
188 2005) and from the Global Aridity Index database (Zomer et al., 2007; Zomer et al.,
189 2008; Trabucco and Zomer, 2009). Though there is a recent update to WorldClim

190 (WorldClim 2: Fick and Hijmans, 2017), we use the original because it provides the
191 basis for the data modelled in the Global Aridity Index database. We calculated three
192 complementary measures of rainfall seasonality from the WorldClim database: the
193 percentage of annual precipitation that falls (1) during the coolest quarter of the year
194 (%cold-quarter rainfall: June, July, August), (2) during the warmest quarter of the year
195 (%warm-quarter rainfall: December, January, February), and (3) during the warmest half
196 of the year (%summer rainfall: October through March). The aridity index (AI) reported
197 in the Global Aridity Index database is expressed as:

198

$$199 \text{ AI} = \text{MAP} / \text{MAE}$$

200

201 where MAP is mean annual precipitation and MAE is mean annual evapotranspiration.
202 Higher AI values indicate more humid conditions. While MAP is strongly correlated with
203 AI in our dataset ($r = 0.958$, $p < 0.001$), we focus on AI because many climate proxies,
204 including flora and fauna, are more directly influenced by moisture availability
205 (humidity/aridity) rather than the total amount of precipitation (e.g., Chevalier and
206 Chase, 2016). It is important to note, however, that while AI can be calculated at broad
207 spatial scales, moisture availability is usually much more heterogeneous than these
208 calculations suggest. Even modest topographic variability can significantly disperse or
209 concentrate surface and groundwater resources, creating substantial micro-
210 topographical differences in moisture availability within regions of similar MAP/MAE.

211 We use canonical correspondence analysis (CCA) to relate the taxonomic

212 composition of the modern assemblages to precipitation seasonality (%warm-quarter

213 and %cold-quarter rainfall) and aridity. CCA is a constrained ordination approach in
214 which faunal assemblages are ordinated relative to one or more known environmental
215 variables, and the species abundances are considered a response to the environmental
216 gradient (Legendre and Legendre, 2012). When the primary axes are plotted in a
217 bivariate plot, assemblages from similar climate regimes will plot close to each other,
218 and the species will plot nearest to those assemblages in which they are most
219 abundant. We then input the Quaternary fossil assemblages into the CCA as
220 supplementary points; these are points that are projected in the same multivariate
221 space as the modern assemblages, but they have no influence on the original
222 ordination. Because the ordination of modern assemblages in the CCA is designed to
223 track environmental variables (the extent to which this is so is examined below), this
224 allows us to interpret ordination scores of fossil assemblages in terms of precipitation
225 seasonality and aridity. We exclude singleton taxa (i.e., those that occur in only one
226 assemblage) from the analysis, as they can disproportionately influence the ordination
227 (Legendre and Legendre, 2012). All fossil assemblages with sample sizes greater than
228 10 individuals are included in the analysis (assemblage LOH from Boomplaas Cave and
229 Layer 3 from Byneskranskop 1 are excluded).

230 The use of CCA allows us to consider the environmental implications of all taxa
231 simultaneously, in contrast to traditional paleoenvironmental inferences derived from
232 (potentially subjective) interpretations of a select handful of indicator taxa. However, it is
233 important to note an assumption that is central to our approach, or indeed any
234 technique that links the taxonomic composition of faunal assemblages to climate or
235 environment. We assume that the target variables (rainfall seasonality and aridity) are

236 important determinants of taxonomic composition (e.g., Birks, 1995). Violation of this
237 assumption translates to reduced accuracy of the environmental reconstruction (e.g., Le
238 and Shackleton, 1994). Though our primary interests concern aridity and rainfall
239 seasonality, we recognize that the presence and abundance of a species in a given
240 assemblage is likely mediated by multiple climatic or environmental variables. For
241 example, some species may indicate highly localized environments (e.g., dense
242 vegetation along a water course) irrespective of variation in our target environmental
243 variables. To enhance compliance with this assumption, we implemented a protocol to
244 ensure analysis of those taxa that are relatively unambiguous indicators of rainfall
245 seasonality or aridity. In particular, we eliminated taxa that are often found in both
246 winter- or summer-dominated rainfall regimes and in relatively humid or arid climates.
247 To do so, we calculated the interquartile range (IQR: 25th to 75th percentile) of
248 %summer rainfall and AI values that characterize the modern assemblages in which a
249 given taxon is found (see Supplemental Table 3). We excluded those taxa ($n = 16$)
250 whose IQRs encompass intermediate values of rainfall seasonality and aridity, defined
251 here as 50% summer rainfall and an AI value of 0.40; the former represents the
252 threshold separating assemblages that receive more winter or more summer rainfall,
253 and the latter represents the midpoint of the range of AI values in the modern sample
254 (from 0.05 to 0.75). Not only are the excluded taxa ambiguous indicators of our target
255 environmental variables (e.g., because they occur in relatively humid or arid climates),
256 but they also tend to have relatively broad tolerances with respect to rainfall seasonality
257 and aridity. The median IQRs of %summer rainfall (46%) and AI values (0.29) of
258 excluded taxa are considerably larger than those of taxa included in analysis (%summer

259 rainfall: 16%; AI: 0.14). In other words, excluded taxa are found in modern assemblages
260 characterized by a much broader range of seasonality and AI values than those
261 retained for analysis.

262 Though it is possible to use these and related analytical approaches to generate
263 numerical reconstructions of past climate (e.g., the aridity index at time X was 0.45)
264 (Birks, 1995), we emphasize ordinal-scale trends here (e.g., more/less arid) to avoid
265 generating results that are seemingly precise but potentially inaccurate. There are
266 several reasons for doing so. First, our assumptions concerning the taphonomic
267 histories of the fossil assemblages reinforce the need for conservative interpretation of
268 the fossil data. Second, taxonomic abundances from fossil mammal assemblages—
269 typically quantified according to MNI or the number of identified specimens (NISP)—
270 often behave in a manner that is ordinal-scale (Grayson, 1984; Lyman, 2008). And
271 lastly, we note that the analyzed fossil assemblages are time-averaged by amounts
272 ranging from hundreds to thousands of years. The precision implied by numerical
273 paleoclimate reconstructions is of questionable accuracy considering that the relatively
274 coarse temporal resolution of the fossil assemblages means they are likely to sample
275 short-term climatic fluctuations. It is for this reason—specifically, the need to ensure that
276 we ask paleoclimatic questions that can be answered given the temporal resolution of
277 the fossil data (e.g., Lyman, 2017)—that we also emphasize long-term paleoclimatic
278 trends (e.g., from the LGM to the onset of the Holocene), highlighting shorter-term
279 climate phenomena only when we have sufficient resolution to do so.

280 RESULTS

281 Modern assemblages

282 Figure 3 plots the ordination of sites and species along the first two axes of the CCA.
283 For the sake of clarity, site names are omitted and they are instead coded by
284 precipitation regime (WRZ, SRZ, and ARZ) and UNEP aridity classification (arid, semi-
285 arid, dry sub-humid, humid). Only those species present in the fossil assemblages are
286 illustrated here. Full details concerning the CCA ordination scores for sites and taxa are
287 provided in Supplementary Table 4.

288 The first axis (axis 1) accounts for 54.8% of the inertia (~variation in taxonomic
289 composition), and it broadly tracks precipitation seasonality. Sites and species with
290 negative values are associated with a greater percentage of warm-quarter rainfall and
291 those with positive values are associated with a greater percentage of cold-quarter
292 rainfall. This relationship is further illustrated in Figure 4A, which plots the axis 1 scores
293 for a given site against %summer rainfall. There is a strong and significant inverse
294 correlation between the two variables ($r = -0.880$, $p < 0.001$). The second axis of the
295 CCA accounts for 45.1% of the inertia and tracks the aridity index (Fig. 3). Sites and
296 species associated with more humid environments tend to have negative axis 2 scores,
297 whereas those associated with arid settings tend to have positive axis 2 scores. This is
298 also shown in Figure 4B, which plots axis 2 scores against the logarithm of the aridity
299 index. The correlation is strong and highly significant ($r = -0.859$, $p < 0.001$).

300

301

302 **Fossil assemblages**

303 The previous analysis indicates that we can use the ordination of assemblages along
304 the first two axes to track ordinal-scale change in rainfall seasonality and aridity in the
305 fossil record. Figure 5 plots the fossil assemblages in the same multivariate space as
306 the modern assemblages. Though sample size can potentially influence such analyses
307 because larger samples translates to recovery of more species (Grayson, 1984; Lyman,
308 2008), which could potentially include species with a disproportionate effect on the
309 ordination, this is not the case here; for the two sites with long stratified microfaunal
310 sequences (Boomplaas and Byneskranskop 1), assemblage sample size is not related
311 to axis 1 and 2 scores (Spearman's rho: $p > 0.15$ for all correlations).

312

313 Boomplaas Cave

314 The Boomplaas Cave assemblages show substantial variation along both axes (Figs. 5-
315 7). From the base of the sequence to the end of the LGM (layer GWA), increasing axis
316 1 scores suggests increasing winter rainfall (Spearman's rho: $r_s = -0.857$, $p = 0.007$).
317 Axis 2 scores remain relatively low (= humid) and stable at this time. The last glacial-
318 interglacial transition (LGIT: layers CL3 to BRL6) is associated with considerably lower
319 axis 1 scores and a significant temporal increase in axis 2 scores ($r_s = 1.000$, $p =$
320 0.017), suggesting enhanced summer rainfall and increasing aridity relative to the LGM.
321 The shift towards more arid conditions peaks in the earliest Holocene (BRL5), with
322 conditions becoming more humid thereafter (declining axis 2 scores from BRL5 to DGL:
323 $r_s = -1.000$, $p < 0.001$). The increase in humidity through the Holocene is associated

324 with increased influence of summer rains (declining axis 1 scores from BRL5 to DGL: –
325 0.893, $p = 0.012$).

326

327 *Nelson Bay Cave*

328 The availability of only two assemblages from Nelson Bay Cave precludes an
329 analysis of temporal change, but they do speak to LGM conditions on the south coastal
330 plains—though the coastline was far from the site at this time (Van Andel, 1989; Fisher
331 et al., 2010)—relative to the other fossil samples. As indicated in Figure 5, both
332 assemblages from this site have positive axis 1 scores that are comparable to or greater
333 than the LGM assemblages from Boomplaas and those from Byneskranskop 1. Though
334 we lack a Holocene comparison from Nelson Bay Cave, this is consistent with
335 enhanced winter rains during the LGM, especially considering the similarities in axis 1
336 scores with a south coast site that is today in the WRZ (Byneskranskop 1). The axis 2
337 scores are more positive than those from the LGM at Boomplaas Cave, implying drier
338 conditions on the south coastal plains relative to the Swartberg range.

339

340 *Byneskranskop 1*

341 The Byneskranskop 1 assemblages show relatively muted variation along the first and
342 second axes of the CCA (Figs. 5-7). There are no clear directional changes across the
343 LGIT (Layers 19-15; Fig. 6), though there is considerable variation within the Holocene
344 (Figs. 6, 7). This variation includes a brief humid pulse associated with increased
345 influence of summer rainfall in the earliest Holocene (Figs. 6, 7). We also observe a
346 steady and statistically significant increase in humidity (declining axis 2 scores: $r_s = -$

347 0.900, $p < 0.001$) coupled with increasing summer rainfall (declining axis 1 scores: $r_s = -$
348 0.636, $p = 0.032$) from layer 12 (~8.5 kcal BP) through to the top of the sequence. To
349 the extent that the uppermost assemblage signals climates similar to the present, we
350 infer that the influence of summer rainfall has been similar to or less than today,
351 implying dominance of winter rainfall throughout the last 17 ka.

352

353

354

355 **DISCUSSION**

356 Our analyses differ from previous studies of southern Cape micromammal assemblages
357 in that they are informed by a large sample of modern assemblages, which provides an
358 empirical link between taxonomic composition and climate (see also Campbell et al.,
359 2011; Campbell et al., 2012). The strong relationships between taxonomic composition
360 and climate documented in our analysis (Fig. 4) enhance confidence that our
361 interpretations of the fossil record are reflecting changes in the target environmental
362 variables. Particularly important are the high coefficients of determination (r^2) for the
363 correlations involving rainfall seasonality (axis 1 and %summer rainfall: $r^2 = 0.775$) and
364 aridity (axis 2 and AI: $r^2 = 0.738$), which together imply that the majority of variance in
365 taxonomic composition of the modern assemblages is related to the target climatic
366 variables. It follows that even though barn owl assemblages provide highly localized
367 representations of the micromammal community (within a 2-3 km radius), they are still
368 highly sensitive to larger-scale climate parameters, at least over the spatial scales
369 examined here. Though the microfaunal record is not as well-resolved as some other

370 climate records from the region, namely those provided by hyrax middens (e.g., Chase
371 et al., 2015b, 2018), speleothems (e.g., Talma and Vogel, 1992), and lake cores (e.g.,
372 Quick et al., 2015, 2016), it does provide a valuable, and compared to many archives,
373 unique, opportunity to simultaneously explore shifts in both moisture availability and
374 rainfall seasonality.

375

376 **Change in the ARZ**

377 The Boomplaas Cave record contributes to an increasingly coherent picture concerning
378 late Quaternary variation in temperate (winter rains) and tropical (summer rains)
379 precipitation systems in what is today the ARZ. It attests to increasing influence of
380 winter rains after ~60 ka, with the strongest winter rainfall signal occurring immediately
381 before and during the LGM (Fig. 6). The Nelson Bay Cave record is consistent with this
382 trend, providing a strong winter rainfall signal in the two samples dating from 23.5 to
383 16.3 kcal BP (Fig. 5).

384 Enhanced winter rains during the LGM is consistent with recent inferences
385 derived from the Boomplaas microfauna (Thackeray and Fitchett, 2016) and with stable
386 carbon ($\delta^{13}\text{C}$) isotopes from Boomplaas grazers (Sealy et al., 2016). The latter indicate
387 abundant C_3 grass during the LGM; because the proportion of C_3 and C_4 grasses in
388 South Africa tracks the influence of winter and summer rains (Vogel et al., 1978), this is
389 consistent with greater influence of winter rainfall. Likewise, the expansion of grassland
390 implied by the Boomplaas micromammals (Avery, 1982) and larger mammals (Klein,
391 1983; Faith, 2013a), together with the strong C_3 signature in the nearby (~3 km east)
392 Cango Caves speleothem (Talma and Vogel, 1992), is also indicative of abundant C_3

393 grasses and winter rains at this time. Further afield at Seweweekspoort, in the Swartberg
394 range 70 km west of Boomplaas (Fig. 1), the combination of elevated grass pollen and
395 reduced $\delta^{13}\text{C}$ in a series of hyrax middens suggests that most rain fell during the winter
396 (Chase et al., 2017, 2018) (Fig. 7D). A potential discrepancy is provided by Sealy's
397 (1996) analysis of $\delta^{13}\text{C}$ in grazers from Nelson Bay Cave. She interpreted stasis in the
398 $\delta^{13}\text{C}$ values of *Syncerus caffer* and *Hippotragus* spp. through the sequence as evidence
399 for stability in the influence of summer and winter rainfall regimes. However, we note
400 that this signal may be influenced by east-west migration of ungulate grazers along the
401 paleo-Agulhas plain during the LGM (Marean, 2010; Faith and Thompson, 2013,
402 Copeland et al., 2016), which would imply that their $\delta^{13}\text{C}$ signatures are not indicative of
403 local vegetation or rainfall regimes.

404 .

405 At Boomplaas Cave, the LGIT (CL3 to BRL6) is associated with enhanced
406 summer rainfall relative to the LGM. (Fig. 6). This is also evident in the Seweweekspoort
407 $\delta^{13}\text{C}$ record, which documents an increase in C_4 vegetation through the LGIT (Fig. 7D).
408 The increasing influence of summer rains broadly tracks changes in summer rainfall
409 inferred from a recent statistical analysis of pollen archives in the interior (SRZ) of
410 southern Africa (Chevalier and Chase, 2015) (Fig. 7A). At the same time, the declining
411 influence of winter rains also tracks the decline in Antarctic sea-ice extent inferred from
412 sea salt sodium flux from the EDML ice core (Fischer et al., 2007; Fig. 7H), consistent
413 with the hypothesis that winter rains are linked to the expansion and contraction of
414 Antarctic sea ice and its effect on the position of the southern westerlies (e.g., van

415 Zinderen Bakker, 1976; Stuut et al., 2004; Chase and Meadows, 2007; Chase et al.,
416 2013, 2017).

417 In contrast to the coherent picture concerning rainfall seasonality provided by
418 southern Cape paleoclimate archives, there is substantial disagreement about variation
419 in moisture availability from the ARZ (e.g., Avery, 1982; Deacon et al., 1984; Scholtz,
420 1986; Deacon and Lancaster, 1988; Avery, 2004; Chase and Meadows, 2007; Faith,
421 2013a, b; Chase et al., 2017, 2018). Our results contribute to a growing body of
422 evidence suggesting a transition from a relatively humid LGM to a more arid Holocene
423 (e.g., Faith 2013a, b; Chase et al., 2017, 2018). The increase in aridity from the LGM to
424 the early Holocene at Boomplaas Cave (Fig. 7C) broadly parallels the $\delta^{15}\text{N}$ record from
425 the Seweweekspoort hyrax middens (Chase et al., 2017, 2018; Fig. 7E). These records
426 are out of phase with the pollen-derived precipitation record from the SRZ (Chevalier
427 and Chase, 2015; Fig. 7A), consistent with the expected inverse relationship between
428 temperate and tropical systems over orbital time-scales (Chase et al., 2017).

429 The relatively humid conditions observed during the LGM persist until ~15 ka,
430 with conditions becoming increasingly arid thereafter (Fig. 6, 7C). We argue that
431 increased evapotranspiration due to warmer temperatures is largely responsible for
432 aridification from 15 ka to the end of the Pleistocene (Fig. 7C). This is suggested by a
433 lack of evidence for changes in rainfall seasonality at Boomplaas Cave (Fig. 7B),
434 together with an absence of prominent directional shifts in SRZ precipitation (Fig. 7A) or
435 Antarctic sea ice (Fig. 7H) over this interval, implying little net change in the strength of
436 tropical or temperate precipitation systems. The aridification trend peaks in the earliest
437 Holocene (Fig. 6, 7C), which represents the most arid portion of the sequence. There is

438 no evidence in the Boomplaas Cave record for the humid pulse seen at
439 Seweweekspoort at ~11 ka (Fig. 7E), but in the absence of better age control for the
440 early Holocene portion of the sequence we cannot rule out the possibility that
441 Boomplaas lacks deposits that sample this relatively short-lived episode or that time-
442 averaging may have muted the signal.

443 The phase of early Holocene aridity documented in the micromammal record is
444 followed by increasingly humid conditions coupled with a moderate increase in the
445 proportion of summer rain (Fig. 6). The Seweweekspoort $\delta^{15}\text{N}$ record lacks a
446 comparable directional change in moisture availability, but it does indicate an increase
447 in grass pollen (Chase et al., 2018) in conjunction with a stronger C_4 signature from the
448 early Holocene until ~ 2 ka (Fig. 7D). An increase in C_4 grasses is also evident in the
449 Cango Caves speleothem for the latter half of the Holocene (there is no record for the
450 first half) (Talma and Vogel, 2013). The combination of evidence from these three
451 archives implies enhanced summer rainfall in the region. Greater rainfall in the warmest
452 portion of the year is likely to promote expansion of shallow-rooting vegetation, including
453 C_4 grasses. Why this increase in summer rainfall is associated with greater humidity at
454 Boomplaas but not at Seweweekspoort is not immediately clear. Resolving this
455 discrepancy will require, among other things, additional records from the ARZ.

456 **Change in the WRZ**

457 The Byneskranskop 1 micromammals provide relatively little evidence for major
458 changes in rainfall seasonality (e.g., compared to Boomplaas Cave), implying a
459 dominance of winter rains over the last 17 ka (Fig. 6). This is not surprising given that
460 the site is located far west of the Indian Ocean moisture source responsible for summer

461 rains. In terms of both seasonality and aridity, there are no clear directional changes
462 across the LGIT (Layers 16-19: Fig. 6). Rather, changes within the Holocene (Layers
463 15-1) are more pronounced than those occurring across the Pleistocene-Holocene
464 transition. The earliest Holocene (Layer 14) is associated with humid conditions (low
465 axis 2 scores), corresponding closely with a similar humid pulse documented in the
466 Seweweekspoort record (Chase et al., 2017, 2018), where it dates from 11.8 to 10.7
467 kcal BP (Fig. 9E). The mechanisms underpinning this humid phase have been
468 suggested to relate to an increase in tropical influence (Chase et al., 2017), and this is
469 clearly reflected in the micromammalian assemblage by reduced axis 1 scores (Figs. 8,
470 9).

471 Following the brief humid phase in the earliest Holocene, we observe a relatively
472 arid middle Holocene—with the driest conditions occurring in Layer 12 (8.7-8.3 ka)—
473 followed by a gradual return to more humid conditions thereafter (Fig. 6, 7). This arid
474 phase has been attributed to reduced influence of the westerlies (Chase et al., 2017),
475 and numerous records from elsewhere in the WRZ also suggest that the middle
476 Holocene was more arid than what came after (e.g., Klein, 1991; Meadows et al., 1996;
477 Meadows and Baxter, 2001; Chase and Thomas, 2007; Scott and Woodborne, 2007b,
478 a; Klein and Cruz-Uribe, 2016). Avery (1993) previously linked expansion of grasses
479 during the middle Holocene to a less seasonal rainfall regime (i.e., a greater proportion
480 of summer rains), but this is not evident in our analysis, which implies that summer rains
481 were relatively unimportant at this time (Fig. 7F). Though it has been suggested that
482 cooler temperatures and increased westerly influence may account for the more humid
483 late Holocene (e.g., Chase and Meadows, 2007), more recent evidence (Chase et al.,

484 2017) indicates a decrease in westerly influence, and drier conditions at some WRZ
485 sites (Chase et al., 2015a). At Byneskranskop 1, the shift towards mesic conditions
486 beginning ~8 ka (Fig. 7G) is associated with (slightly) greater influence of summer
487 rainfall (Fig. 7F), potentially translating to a less severe summer drought. This is
488 consistent with evidence and inferences drawn from hyrax midden data from the
489 eastern WRZ at Katbakkies Pass (Fig. 1), which indicate that although most rain falls in
490 the winter, variation in overall moisture availability/drought stress is largely determined
491 by the changing influence of summer rains and their effect on the severity of the dry
492 season (see Chase et al., 2015b).

493

494 **CONCLUSIONS**

495 We show that the taxonomic composition of southern African owl-accumulated
496 micromammal assemblages is strongly related to precipitation seasonality and aridity.
497 We use these relationships to infer changes in the late Quaternary precipitation history
498 of the southern Cape from three fossil assemblages. In what is today the ARZ, the
499 micromammal records from Boomplaas Cave and Nelson Bay Cave imply enhanced
500 winter rainfall during glacial Pleistocene, consistent with models suggesting eastward
501 expansion of the WRZ (e.g., van Zinderen Bakker, 1976; Chase and Meadows, 2007;
502 Chase et al., 2017). The Boomplaas Cave record contributes to a growing body of
503 evidence implying a relatively humid LGM, followed by increased aridity across the
504 LGIT.. The WRZ record from Byneskranskop 1 is characterized by relatively little
505 change in rainfall seasonality throughout its sequence. Changes in moisture availability
506 are more pronounced, however, especially during the Holocene. This includes a

507 relatively humid late Holocene, interrupted by a period of aridity during the middle
508 Holocene, consistent with other records from the WRZ. Overall, the coherence between
509 the micromammal record and other local and regional climate proxies (Figs. 9, 10)
510 reinforces the abundant potential of southern African micromammal assemblages as
511 indicators of paleoclimate (Avery, 1983, 1990, 2007). Although generation of new
512 climate archives will be essential to resolving current and emerging questions
513 concerning southern Africa's precipitation history, our analyses show that new analysis
514 of the existing records can also help us get closer to the answers we seek.

515

516

517

518 **ACKNOWLEDGMENTS**

519 An early version of this study was presented at a Society for American Archaeology
520 session organized by Eugene Morin, Arianne Boileau, and Elspeth Ready. The version
521 reported here benefited from several participant comments. We thank the members of
522 the University of Utah Archaeological Center, Curtis Marean (Associate Editor), and two
523 anonymous referees for valuable feedback on an earlier draft. Justin Pargeter kindly
524 shared new radiocarbon dates for Boomplaas Cave prior to their publication. An
525 Australian Research Council (ARC) Discovery Early Career Researcher Award
526 (DE160100030) supported JTF in the early stages of this project.

527

528 **REFERENCES**

529 Andrews, P., 1990. *Owls, Caves, and Fossils*. University of Chicago Press, Chicago.

- 530 Avery, D.M., 1982. Micromammals as palaeoenvironmental indicators and an
531 interpretation of the late Quaternary in the southern Cape Province, South Africa.
532 *Annals of the South African Museum* 85, 183-374.
- 533 Avery, D.M., 1983. Palaeoenvironmental implications of the small Quaternary mammals
534 of the fynbos region, In: Deacon, H.J., Hendey, Q.B., Lambrechts, J.J.N. (Eds.),
535 *Fynbos Palaeoecology: A Preliminary Synthesis*, South African National Scientific
536 Programmes Report No 75. Mills Litho, Cape Town, pp. 139-155.
- 537 Avery, D.M., 1987. Late Pleistocene coastal environment of the southern Cape Province
538 of South Africa: micromammals from Klasies River Mouth. *Journal of Archaeological*
539 *Science* 14, 405-421.
- 540 Avery, D.M., 1990. Holocene climatic change in southern Africa: the contribution of
541 micromammals to its study. *South African Journal of Science* 86, 407-412.
- 542 Avery, D.M., 1992. Ecological data on micromammals collected by barn owls *Tyto alba*
543 in the West Coast National Park, South Africa. *Israel Journal of Zoology* 38, 385-
544 397.
- 545 Avery, D.M., 1993. Last Interglacial and Holocene altithermal environments in South
546 Africa and Namibia: micromammalian evidence. *Palaeogeography,*
547 *Palaeoclimatology, Palaeoecology* 101, 221-228.
- 548 Avery, D.M., 1999. A preliminary assessment of the relationship between trophic
549 variability in southern African Barn owls *Tyto alba* and climate. *Ostrich* 70, 179-186.
- 550 Avery, D.M., 2004. Size variation in the common molerat *Cryptomys hottentotus* from
551 southern Africa and its potential for palaeoenvironmental reconstruction. *Journal of*
552 *Archaeological Science* 31, 273-282.

- 553 Avery, D.M., 2007. Micromammals as palaeoenvironmental indicators of the southern
554 Afrian Quaternary. *Transactions of the Royal Society of South Africa* 62, 17-23.
- 555 Bar-Matthews, M., Marean, C.W., Jacobs, Z., Karkanas, P., Fisher, E.C., Herries, A.I.R.,
556 Brown, K., Williams, H.M., Bernatchez, J., Ayalon, A., Nilssen, P.J., 2010. A high
557 resolution and continuous isotopic speleothem record of paleoclimate and
558 paleoenvironment from 90 to 53 ka from Pinnacle Point on the south coast of South
559 Africa. *Quaternary Science Reviews* 29, 2131-2145.
- 560 Birks, H.J.B., 1995. Quantitative palaeoenvironmental reconstructions, In: Maddy, D.,
561 Brew, J.S. (Eds.), *Statistical Modelling of Quaternary Science Data*. Quaternary
562 Research Association, Technical Guide 5, Cambridge, pp. 161-254.
- 563 Bronk Ramsey, C., 2013. OxCal 4.2 <http://c14.arch.ox.ac.uk/>.
- 564 Campbell, T.L., Lewis, P.J., Thies, M.L., Williams, J.K., 2012. A Geographic Information
565 Systems (GIS)-based analysis of modern South African rodent distributions, habitat
566 use, and environmental tolerances. *Ecology and Evolution* 2, 2881-2894.
- 567 Campbell, T.L., Lewis, P.J., Williams, J.K., 2011. Analysis of the modern distribution of
568 South African *Gerbilliscus* (Rodentia: Gerbillinae) with implications for Plio-
569 Pleistocene palaeoenvironmental reconstruction. *South African Journal of Science*
570 107, Article #497, 498 pages.
- 571 Chase, B.M., 2010. South African palaeoenvironments during marine oxygen isotope
572 stage 4: a context for the Howiesons Poort and Still Bay industries. *Journal of*
573 *Archaeological Science* 37, 1359-1366.
- 574 Chase, B.M., Boom, A., Carr, A.S., Carré, M., Chevalier, M., Meadows, M.E., Pedro,
575 J.B., Stager, J.C., Reimer, P.J., 2015a. Evolving southwest African response to

- 576 abrupt deglacial North Atlantic climate change events. *Quaternary Science Reviews*
577 121, 132-136.
- 578 Chase, B.M., Boom, A., Carr, A.S., Meadows, M.E., Reimer, P.J., 2013. Holocene
579 climate change in southernmost South Africa: rock hyrax middens record shifts in
580 the southern westerlies. *Quaternary Science Reviews* 82, 199-205.
- 581 Chase, B.M., Chevalier, M., Boom, A., Carr, A.S., 2017. The dynamic relationship
582 between temperate and tropical circulation systems across South Africa since the
583 last glacial maximum. *Quaternary Science Reviews* 174, 54-62.
- 584 Chase, B.M., Faith, J.T., Mackay, A., Chevalier, M., Carr, A.S., Boom, A., Lim, S.,
585 Reimer, P.J., 2018. Climatic controls on Later Stone Age human adaptation in
586 Africa's southern Cape. *Journal of Human Evolution* 114, 35-44.
- 587 Chase, B.M., Lim, S., Chevalier, M., Boom, A., Carr, A.S., Meadows, M.E., Reimer,
588 P.J., 2015b. Influence of tropical easterlies in southern Africa's winter rainfall zone
589 during the Holocene. *Quaternary Science Reviews* 107, 138-148.
- 590 Chase, B.M., Meadows, M.E., 2007. Late Quaternary dynamics of southern Africa's
591 winter rainfall zone. *Earth-Science Reviews* 84, 103-138.
- 592 Chase, B.M., Quick, L.J. 2018. Influence of Agulhas forcing of climate change in South
593 Africa's southern Cape. *Quaternary Research*.
- 594 Chase, B.M., Thomas, D.S.G., 2007. Multiphase late Quaternary aeolian sediment
595 accumulation in western South Africa: timing and relationship to palaeoclimatic
596 changes inferred from the marine record. *Quaternary International* 166, 29-41.

- 597 Chevalier, M., Chase, B.M., 2015. Southeast African records reveal a coherent shift
598 from high- to low-latitude forcing mechanisms along the east African margin across
599 last glacial–interglacial transition. *Quaternary Science Reviews* 125, 117-130.
- 600 Chevalier, M., Chase, B.M., 2016. Determining the drivers of long-term aridity variability:
601 a southern African case study. *Journal of Quaternary Science* 31, 143-151.
- 602 Clark, P.U., Dyke, A.S., Shakun, J.D., Carlson, A.E., Clark, J., Wohlfarth, B., Mitrovica,
603 J.X., Hostetler, S.W., McCabe, A.M., 2009. The Last Glacial Maximum. *Science*,
604 710-714.
- 605 Cockcroft, M.J., Wilkinson, M.J., Tyson, P.D., 1987. The application of a present-day
606 climate model to the Late Quaternary in southern Africa. *Climatic Change* 10, 161-
607 181.
- 608 Copeland, S.R., Cawthra, H.C., Fisher, E.C., Lee-Thorp, J.A., Cowling, R.M., le Roux,
609 P.J., Hodgkins, J., Marean, C.W., 2016. Strontium isotope investigation of ungulate
610 movement patterns on the Pleistocene Paleo-Agulhas Plain of the Greater Cape
611 Floristic Region, South Africa. *Quaternary Science Reviews* 141, 65-84.
- 612 Cowling, R.M., 1983. Phytochorology and vegetation history in the south-eastern Cape,
613 South Africa. *Journal of Biogeography* 10, 393-419.
- 614 Deacon, H.J., 1979. Excavations at Boomplaas cave - a sequence through the Upper
615 Pleistocene and Holocene in South Africa. *World Archaeology* 10, 241-257.
- 616 Deacon, H.J., Deacon, J., Scholtz, A., Thackeray, J.F., Brink, J.S., 1984. Correlation of
617 palaeoenvironmental data from the Late Pleistocene and Holocene deposits at
618 Boomplaas Cave, southern Cape, In: Vogel, J.C. (Ed.), *Late Cainozoic
619 Palaeoclimates of the Southern Hemisphere*. Balkema, Rotterdam, pp. 339-351.

- 620 Deacon, J., 1984. The Later Stone Age of southernmost Africa. British Archaeological
621 Reports, International Series 213, Oxford.
- 622 Deacon, J., Lancaster, N., 1988. Late Quaternary Palaeoenvironments of Southern
623 Africa. Oxford University Press, New York.
- 624 Faith, J.T., 2013a. Taphonomic and paleoecological change in the large mammal
625 sequence from Boomplaas Cave, Western Cape, South Africa. Journal of Human
626 Evolution 65, 715-730.
- 627 Faith, J.T., 2013b. Ungulate diversity and precipitation history since the Last Glacial
628 Maximum in the Western Cape, South Africa. Quaternary Science Reviews 68, 191-
629 199.
- 630 Faith, J.T., Thompson, J.C., 2013. Fossil evidence for seasonal calving and migration of
631 extinct blue antelope (*Hippotragus leucophaeus*) in southern Africa. Journal of
632 Biogeography 40, 2108-2118.
- 633 Fernández-Jalvo, Y., Andrews, P., Denys, C., Sesé, C., Stoetzel, E., Marin-Monfort, E.,
634 Pesquero, D., 2016. Taphonomy for taxonomists: Implications of predation in small
635 mammal studies. Quaternary Science Reviews 139, 138-157.
- 636 Fick, S.E., Hijmans, R.J., 2017. WorldClim 2: new 1-km spatial resolution climate
637 surfaces for global land areas. International Journal of Climatology.
- 638 Fischer, H., Fundel, F., Ruth, U., Twarloh, B., Wegner, A., Udisti, R., Becagli, S.,
639 Castellano, E., Morganti, A., Severi, M., Wolff, E.W., Littot, G.C., Röthlisberger, R.,
640 Mulvaney, R., Hutterli, M.A., Kaufmann, P.R., Federer, U., Lambert, F., Bigler, M.,
641 Hansson, M.E., Jonsell, U., de Angelis, M., Boutron, C.F., Siggaard-Andersen, M.-L.,
642 Steffensen, J.P., Barbante, C., Gaspari, V., Gabrielli, P., Wagenbach, D., 2007.

- 643 Reconstruction of millennial changes in dust emission, transport and regional sea ice
644 coverage using the deep EPICA ice cores from the Atlantic and Indian Ocean sector
645 of Antarctica. *Earth and Planetary Science Letters* 260, 340-354.
- 646 Fisher, E.C., Bar-Matthews, M., Jerardino, A., Marean, C.W., 2010. Middle and Late
647 Pleistocene paleoscape modeling along the southern coast of South Africa.
648 *Quaternary Science Reviews* 29, 1382-1398.
- 649 Grayson, D.K., 1984. *Quantitative Zooarchaeology*. Academic Press, Orlando, Florida.
- 650 Happold, D., 2013. *Mammals of Africa. Volume III: Rodents, Hares and Rabbits*.
651 Bloomsbury Publishing, London.
- 652 Happold, M., Happold, D., 2013. *Mammals of Africa. Volume IV: Hedgehogs, Shrews
653 and Bats*. Bloomsbury Publishing, London.
- 654 Heine, K., 1982. The main stages of the late Quaternary evolution of the Kalahari
655 region, southern Africa. *Palaeoecology of Africa* 15, 53-76.
- 656 Hijmans, R.J., Cameron, S.E., Parra, J.L., Jones, P.G., Jarvis, A., 2005. Very high
657 resolution interpolated climate surfaces for global land areas. *International Journal of
658 Climatology* 25, 1965-1978.
- 659 Hogg, A.G., Hua, Q., Blackwell, P.G., Niu, M., Buck, C.E., Guilderson, T.P., Heaton,
660 T.J., Palmer, J.G., Reimer, P.J., Reimer, R.W., Turney, C.S.M., Zimmerman, S.R.H.,
661 2013. SHCal13 Southern Hemisphere Calibration, 0–50,000 Years cal BP.
662 *Radiocarbon* 55, 1889-1903.
- 663 Inskeep, R.R., 1987. *Nelson Bay Cave, Cape Province, South Africa: the Holocene
664 levels*. BAR International Series 357, Oxford.

- 665 Klein, R.G., 1972. Preliminary report on the July through September 1970 excavations
666 at Nelson Bay Cave, Plettenberg Bay (Cape Province, South Africa). *Palaeoecology*
667 of Africa 6, 177-208.
- 668 Klein, R.G., 1983. Palaeoenvironmental implications of Quaternary large mammals in
669 the fynbos region, In: Deacon, H.J., Hendey, Q.B., Lambrechts, J.J.N. (Eds.),
670 Fynbos Palaeoecology: A Preliminary Synthesis, South African National Scientific
671 Programmes Report No 75. Mills Litho, Cape Town, pp. 116-138.
- 672 Klein, R.G., 1991. Size variation in Cape dune mole rat (*Bathyergus suillus*) and late
673 Quaternary climatic change in the southwestern Cape Province, South Africa.
674 *Quaternary Research* 36, 243-256.
- 675 Klein, R.G., Cruz-Uribe, K., 2016. Large mammal and tortoise bones from Elands bay
676 Cave (South Africa): implications for Later Stone Age environment and ecology.
677 *South African Humanities* 29, 259-282.
- 678 Le, J., Shackleton, N.J., 1994. Reconstruction paleoenvironment by transfer function:
679 model evaluation with simulated data. *Marine Micropaleontology* 24, 187-199.
- 680 Legendre, P., Legendre, L., 2012. *Numerical Ecology*. Elsevier, New York.
- 681 Loftus, E., Sealy, J., Lee-Thorp, J., 2016. New radiocarbon dates and Bayesian models
682 for Nelson Bay Cave and Byneskranskop 1: implications for the South African Later
683 Stone Age sequence. *Radiocarbon* 58, 365-381.
- 684 Lyman, R.L., 2008. *Quantitative Paleozoology*. Cambridge University Press,
685 Cambridge.
- 686 Lyman, R.L., 2012. The influence of screen mesh size, and size and shape of rodent
687 teeth on recovery. *Journal of Archaeological Science* 39, 1854-1861.

- 688 Lyman, R.L., 2017. Paleoenvironmental reconstruction from faunal remains: ecological
689 basics and analytical assumptions. *Journal of Archaeological Research* 25, 315-371.
- 690 Marean, C.W., 2010. Pinnacle Point Cave 13B (Western Cape Province, South Africa)
691 in context: The Capr Floral kingdom, shellfish, and modern human origins. *Journal of*
692 *Human Evolution* 59, 425-443.
- 693 Marean, C.W., Cawthra, H.C., Cowling, R.M., Esler, K.J., Fisher, E., Milewski, A., Potts,
694 A.J., Singels, E., De Vynck, J., 2014. Stone Age people in a changing South African
695 Greater Cape Floristic Region, In: Allsopp, N., Colville, J.F., Verboom, G.A. (Eds.),
696 *Fynbos: Ecology, Evolution, and Conservation of a Megadiverse Region*. Oxford
697 University Press, Oxford, pp. 164-199.
- 698 Matthews, T., Rector, A.L., Jacobs, Z., Herries, A.I.R., Marean, C.W., 2011.
699 Environmental implications of micromammals accumulated close to the MIS 6 to MIS
700 5 transition at Pinnacle Point Cave 9 (Mossel Bay, Western Cape Province, South
701 Africa). *Paleogeography, Paleoclimatology, Paleoecology* 302, 213-229.
- 702 Meadows, M.E., Baxter, A.J., 2001. Holocene vegetation history and
703 palaeoenvironments at Klaarfontein Springs, Western Cape, South Africa. *The*
704 *Holocene* 11, 699-706.
- 705 Meadows, M.E., Baxter, A.J., Parkington, J., 1996. Late Holocene environments at
706 Verlorenvlei, Western Cape Province, South Africa. *Quaternary International* 33, 81-
707 95.
- 708 Nel, T.H., Henshilwood, C.S., 2016. The small mammal sequence from the c. 76 – 72
709 ka Still Bay levels at Blombos Cave, South Africa – Taphonomic and
710 palaeoecological implications for human behaviour. *PLoS ONE* 11, e0159817.

- 711 Nel, T.H., Wurz, S., Henshilwood, C.S., 2018. Small mammals from Marine Isotope
712 Stage 5 at Klasies River, South Africa—Reconstructing the local palaeoenvironment.
713 Quaternary International 471, 6-20.
- 714 Pargeter, J., Loftus, E., Mackay, A., Mitchell, P.J., Stewart, B.A., In Press. New ages
715 from Boomplaas Cave, South Africa, provide increased resolution on late/terminal
716 Pleistocene human behavioural variability. *Azania: Archaeological Research in*
717 *Africa*.
- 718 Parkington, J.E., Cartwright, C., Cowling, R.M., Baxter, A., Meadows, M., 2000.
719 Palaeovegetation at the last glacial maximum in the western Cape, South Africa:
720 wood charcoal and pollen evidence from Elands Bay Cave. *South African Journal of*
721 *Science* 96, 543-546.
- 722 Partridge, T.C., Avery, D.M., Botha, G.A., Brink, J.S., Deacon, J., Herbert, R.S., Maud,
723 R.R., Scholtz, A., Scott, L., Talma, A.S., Vogel, J.C., 1990. Late Pleistocene and
724 Holocene climatic change in southern Africa. *South African Journal of Science* 86,
725 302-306.
- 726 Quick, L.J., Carr, A.S., Meadows, M.E., Boom, A., Bateman, M.D., Roberts, D.L.,
727 Reimer, P.J., Chase, B.M., 2015. A late Pleistocene-Holocene multi-proxy record of
728 palaeoenvironmental change from Still Bay, southern Cape Coast, South Africa.
729 *Journal of Quaternary Science* 30, 870-885.
- 730 Quick, L.J., Meadows, M.E., Bateman, M.D., Kirsten, K.L., Mäusbacher, R., Haberzettl,
731 T., Chase, B.M., 2016. Vegetation and climate dynamics during the last glacial
732 period in the fynbos-afrotemperate forest ecotone, southern Cape, South Africa.
733 *Quaternary International* 404B, 136-149.

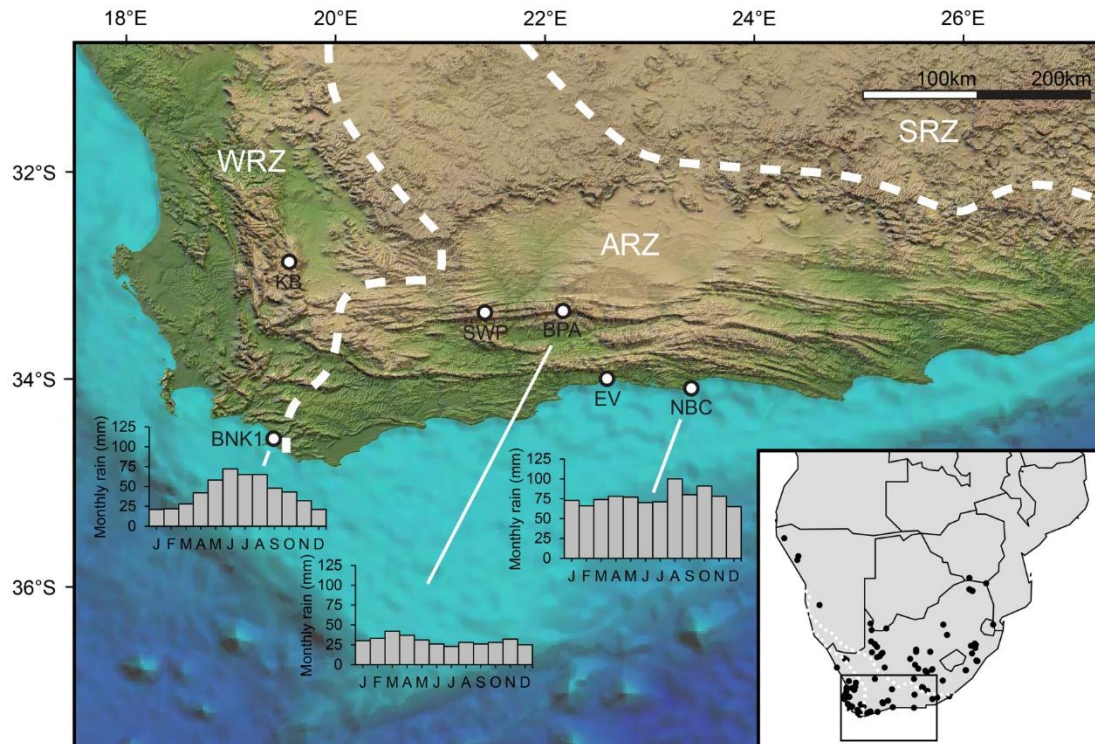
- 734 Reed, D.N., 2005. Taphonomic implications of roosting behavior and trophic habits in
735 two species of African owl. *Journal of Archaeological Science* 32, 1669-1676.
- 736 Scholtz, A., 1986. *Palynological and Palaeobotanical Studies in the Southern Cape*, MA
737 Thesis, University of Stellenbosch, South Africa.
- 738 Schweitzer, F.R., Wilson, M.L., 1982. Byneskranskop 1, a late Quaternary living site in
739 the southern Cape Province, South Africa. *Annals of the South African Museum* 88,
740 1-203.
- 741 Scott, L., Woodborne, S., 2007a. Pollen analysis and dating of late Quaternary faecal
742 deposits (hyraceum) in the Cederberg, Western Cape, South Africa. *Review of*
743 *Paleobotany and Palynology* 144, 123-134.
- 744 Scott, L., Woodborne, S., 2007b. Vegetation history inferred from pollen in Late
745 Quaternary faecal deposits (hyraceum) in the Cape winter-rain region and its
746 bearing on past climates in South Africa. *Quaternary Science Reviews* 26, 941-953.
- 747 Sealy, J., Lee-Thorp, J., Loftus, E., Faith, J.T., Marean, C.W., 2016. Late Quaternary
748 environmental change in the Southern Cape, South Africa, from stable carbon and
749 oxygen isotopes in faunal tooth enamel from Boomplaas Cave. *Journal of*
750 *Quaternary Science* 31, 919-927.
- 751 Sealy, J.C., 1996. Seasonality of rainfall around the last glacial maximum as
752 reconstructed from carbon isotope analyses of animal bones from Nelson Bay Cave.
753 *South African Journal of Science* 92, 441-444.
- 754 Stuut, J.-B.W., Crosta, X., van der Borg, K., Schneider, R.R., 2004. On the relationship
755 between Antartic sea ice and southwestern African climate during the late
756 Quaternary. *Geology* 32, 909-912.

- 757 Talma, A.S., Vogel, J.C., 1992. Late Quaternary palaeotemperatures derived from a
758 speleothem from Cango Caves, Cape Province, South Africa. *Quaternary Research*
759 37, 203-213.
- 760 Taylor, I. (1994). *Barn Owls*. Cambridge University Press, Cambridge.
- 761 Thackeray, J.F., 1987. Late Quaternary environmental changes inferred from small
762 mammalian fauna, southern Africa. *Climatic Change* 10, 285-305.
- 763 Thackeray, J.F., 1990. Temperature indices from late Quaternary sequences in South
764 Africa: comparisons with the Vostok core. *South African Geographic Journal* 72, 47-
765 49.
- 766 Thackeray, J.F., Fitchett, J.M., 2016. Rainfall seasonality captured in micromammalian
767 fauna in Late Quaternary contexts, South Africa. *Palaeontologia Africana* 51, 1-9.
- 768 Trabucco, A., Zomer, R.J., 2009. Global Aridity Index (Global-Aridity) and Global
769 Potential Evapo-Transpiration (Global-PET) Geospatial Database. CGIAR
770 Consortium for Spatial Information, <http://www.cgiar-csi.org/>.
- 771 Tyson, P.D., 1986. *Climatic change and variability in southern Africa*. Oxford University
772 Press, Cape Town.
- 773 UNEP, 1997. *World Atlas of Desertification*. UNEP, London.
- 774 Van Andel, T.H., 1989. Late Pleistocene sea levels and the human exploitation of the
775 shore and shelf of southern South Africa. *Journal of Field Archaeology* 16, 133-155.
- 776 van Zinderen Bakker, E.M., 1967. Upper Pleistocene stratigraphy and Holocene
777 ecology on the basis of vegetation changes in Sub-Saharan Africa, In: Bishop,
778 W.W., Clark, J.D. (Eds.), *Background to Evolution in Africa*. University of Chicago
779 Press, Chicago, pp. 125-157.

- 780 van Zinderen Bakker, E.M., 1976. The evolution of late Quaternary paleoclimates of
781 southern Africa. *Palaeoecology of Africa* 9, 160-202.
- 782 Vogel, J.C., Fuls, A., Ellis, R.P., 1978. The geographical distribution of Kranz grasses in
783 South Africa. *South African Journal of Science* 74, 209-215.
- 784 Wilson, D.E., Reeder, D.M., 2005. *Mammal Species of the World*, 3rd Edition. Johns
785 Hopkins University Press.
- 786 Zomer, R.J., Bossio, D.A., Trabucco, A., Yuanjie, L., Gupta, D.C., Singh, V.P., 2007.
787 *Trees and Water: Smallholder Agroforestry on Irrigated Lands in Northern India*.
788 International Water Management Institute, Columbo, Sri Lanka.
- 789 Zomer, R.J., Trabucco, A., Bossio, D.A., van Straaten, O., Verchot, L.V., 2008. Climate
790 change mitigation: a spatial analysis of global land suitability for clean development
791 mechanism afforestation and reforestation. *Agriculture, Ecosystems and*
792 *Environments* 126, 67-80.
- 793

794 **FIGURE CAPTIONS**

795

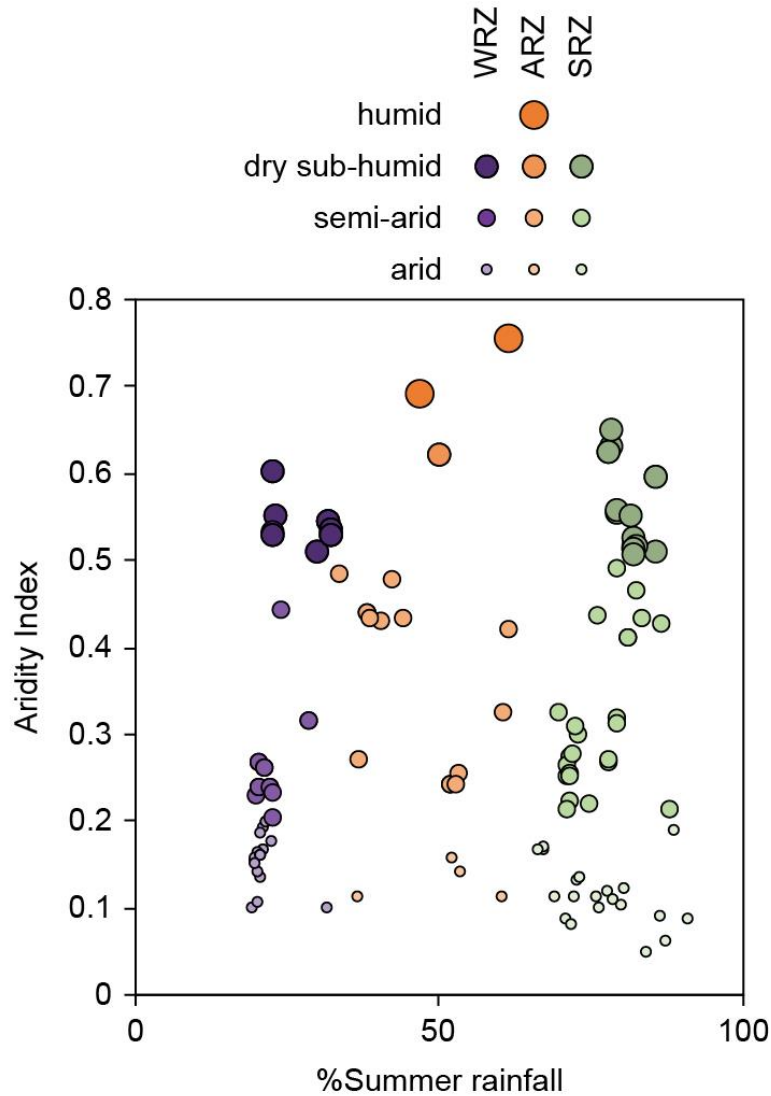


796

797

798 **Figure 1.** The location of the three fossil sites examined here, with monthly rainfall
 799 totals (data from Hijmans et al. 2005), and other sites discussed in the text. BNK1 =
 800 Byneskranskop 1; BPA = Boomploas Cave; KB = Katbakkies Pass; NBC = Nelson Bay
 801 Cave; SWP = Seweweekspoort. Inset: The location of 123 modern microfaunal samples
 802 across southern Africa. Dashed white lines denote boundaries of winter rainfall zone
 803 (WRZ), aseasonal rainfall zone (ARZ), and summer rainfall zone (SRZ).

804



805

806

807 **Figure 2.** The percentage of summer rainfall (% of rainfall from October to March) and

808 aridity index (AI) values (= MAP / MAE; from Zomer et al., 2007; Zomer et al., 2008;

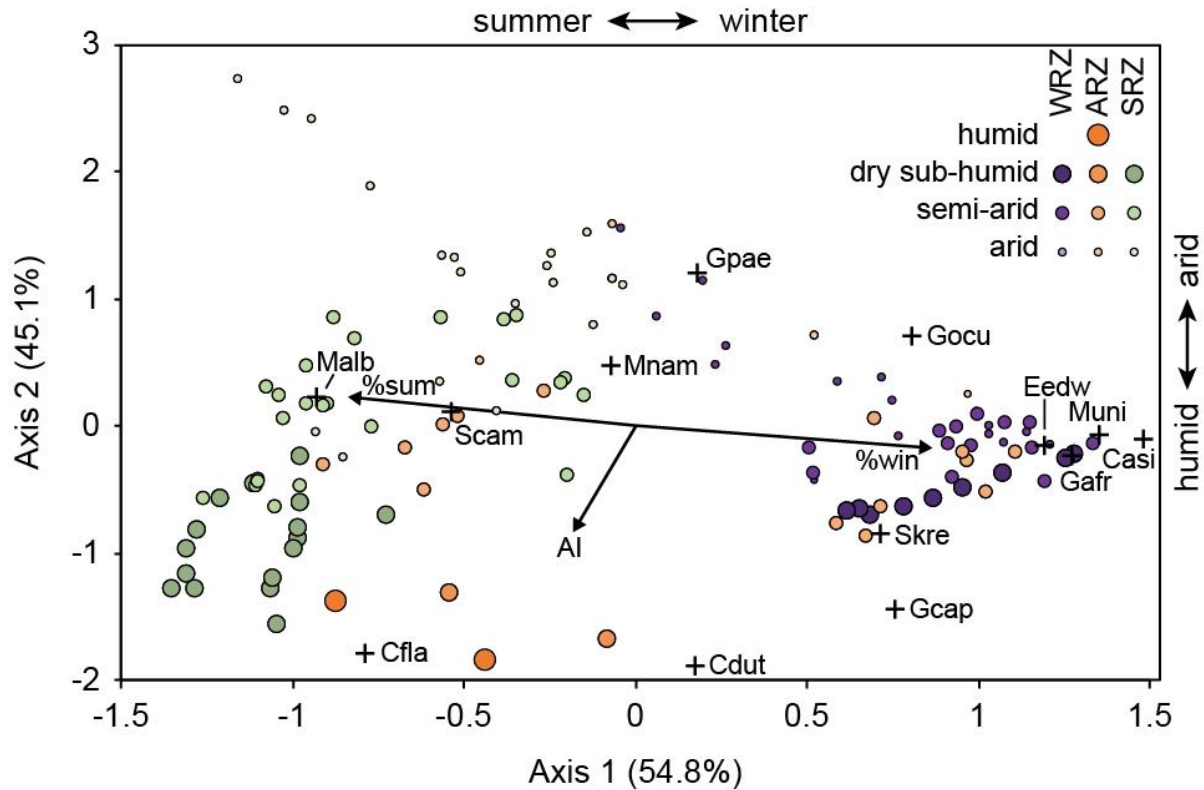
809 Trabucco and Zomer, 2009) of the 123 modern microfauna samples. Higher AI values

810 indicate more humid conditions. Humid = AI > 0.65; Dry sub-humid = 0.5 < AI < 0.65;

811 Semi-arid = 0.2 < AI < 0.5; Arid = 0.05 < AI < 0.2. WRZ = winter rainfall zone; ARZ =

812 aseasonal rainfall zone; SRZ = summer rainfall zone.

813



814

815

816 **Figure 3.** Ordination of modern assemblages (circles) and taxa (+) along the first two

817 axes of the CCA. Arrows indicate vectors for the aridity index (AI), %warm-quarter

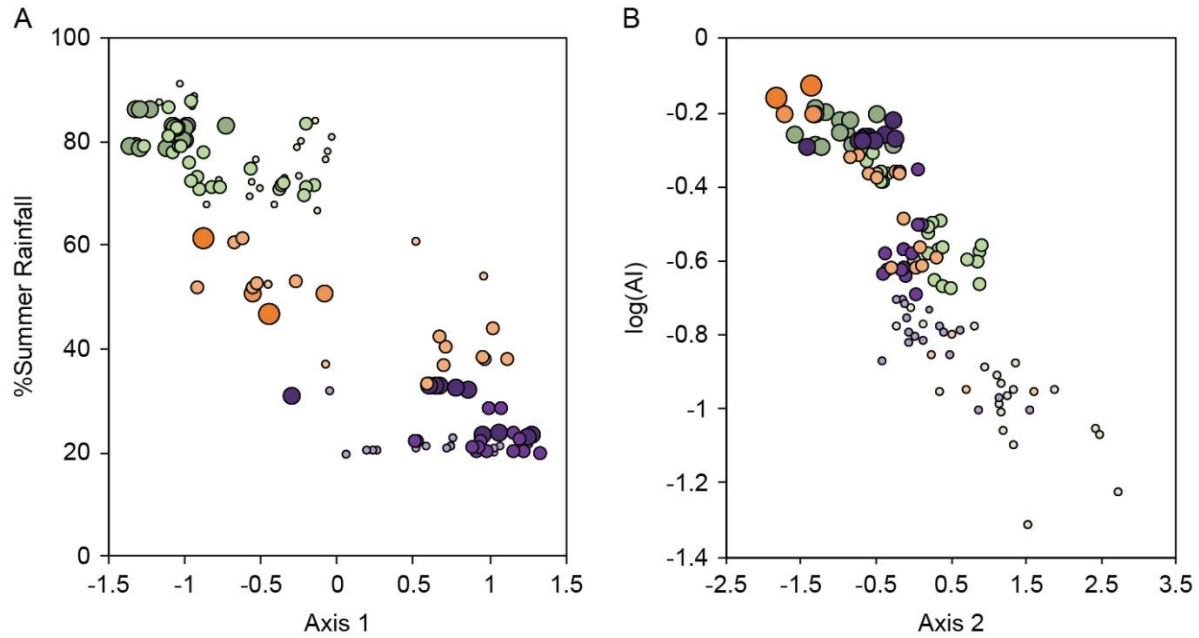
818 rainfall (%sum), and %cold-quarter rainfall (%win). For the sake of clarity, only those

819 taxa occurring in the late Quaternary fossil samples are illustrated here (see

820 Supplementary Table 4 for all taxa). Species abbreviations are as follows: Cdut =

821 *Chlorotalpa duthiae*; Casi = *Chrysochloris asiatica*; Cfla = *Crocidura flavescens*; Eedw =822 *Elephantulus edwardii*; Gcap = *Georychus capensis*; Gafr = *Gerbilliscus afra*; Gpae =823 *Gerbillurus paebe*; Gocu = *Graphiurus ocellaris*; Malb = *Mystromys albicaudatus*; Mnam824 = *Micaleamys namaquensis*; Muni = *Myotomys unisulcatus*; Scam = *Saccostomus*825 *campestris*; Skre = *Steatomys krebsii*

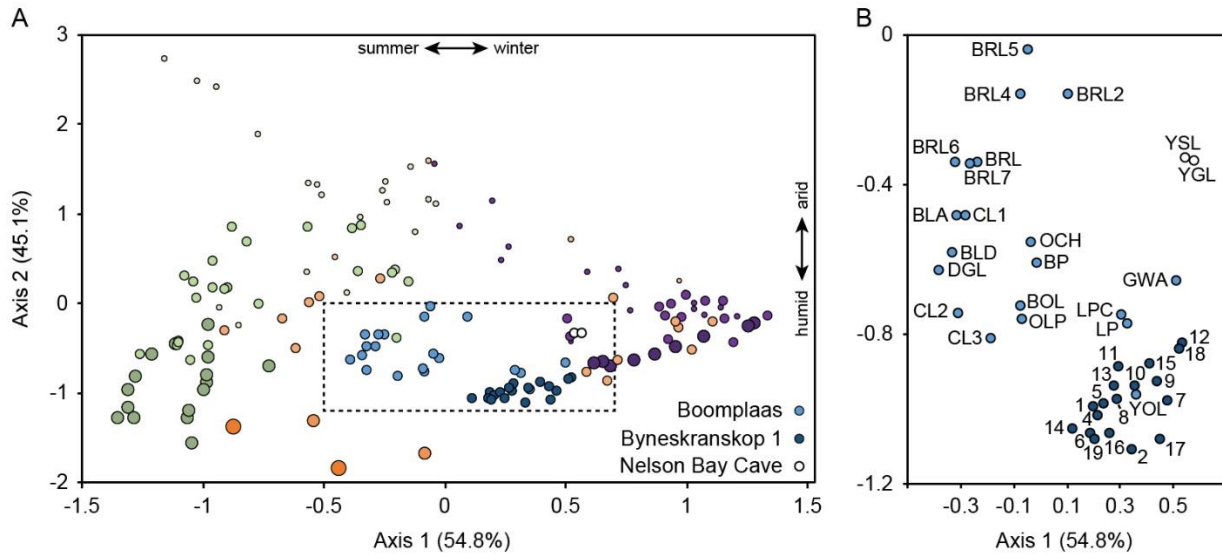
826



827

828 **Figure 4.** (A) The relationship between Axis 1 and the %summer rainfall, and (B) the
 829 relationship between Axis 2 and the logarithm of the aridity index (AI) across the 123
 830 modern microfaunal assemblages. Symbol legend for modern assemblages follows
 831 Figure 2 (green = SRZ; orange = ARZ; purple = WRZ; larger symbols = more humid;
 832 smaller symbols = more arid).

833



834

835 **Figure 5.** (A) Ordination of fossil assemblages relative to the modern assemblages.

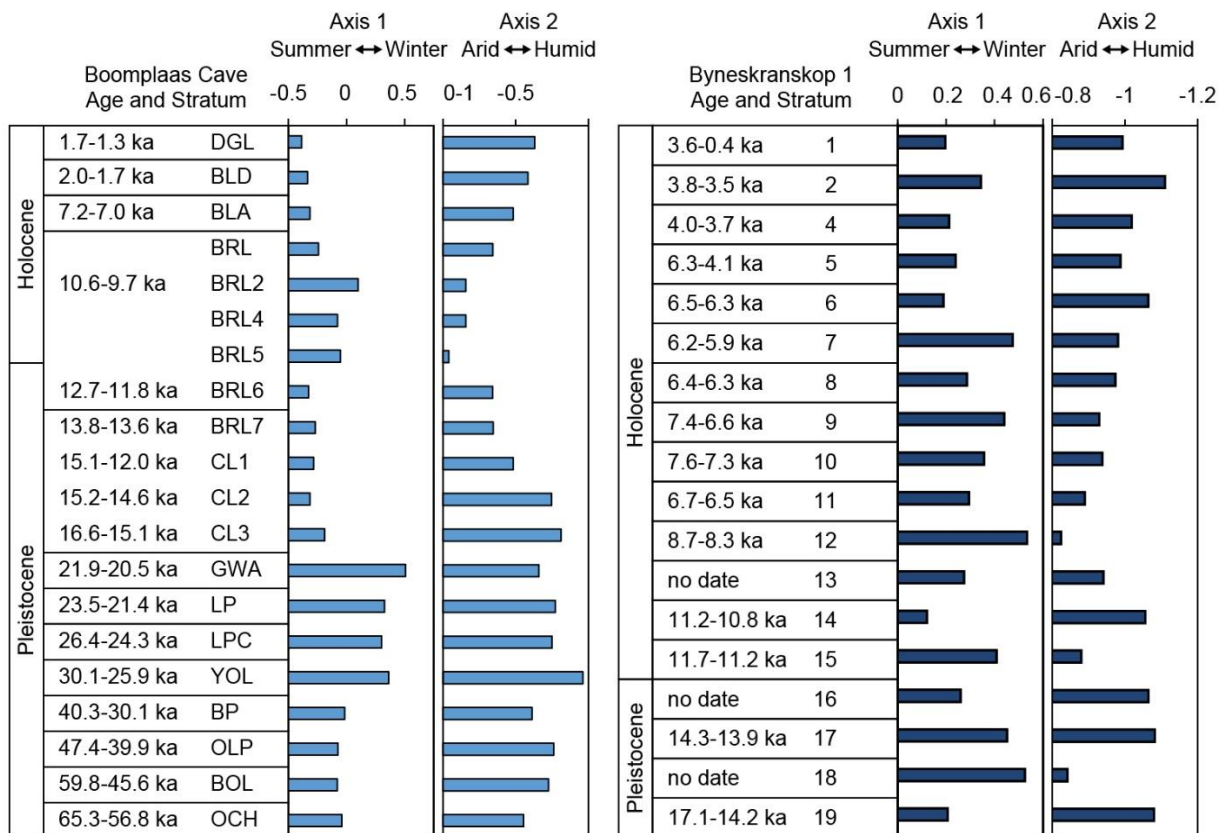
836 Symbol for modern assemblages follows Figure 2 (green = SRZ; orange = ARZ; purple

837 = WRZ; larger symbols = more humid; smaller symbols = more arid). Box

838 encompassing fossil assemblages shown in B, with modern assemblages removed for

839 clarity.

840



841

842 **Figure 6.** Axis 1 (rainfall seasonality) and axis 2 (aridity) scores through the Boomplaas

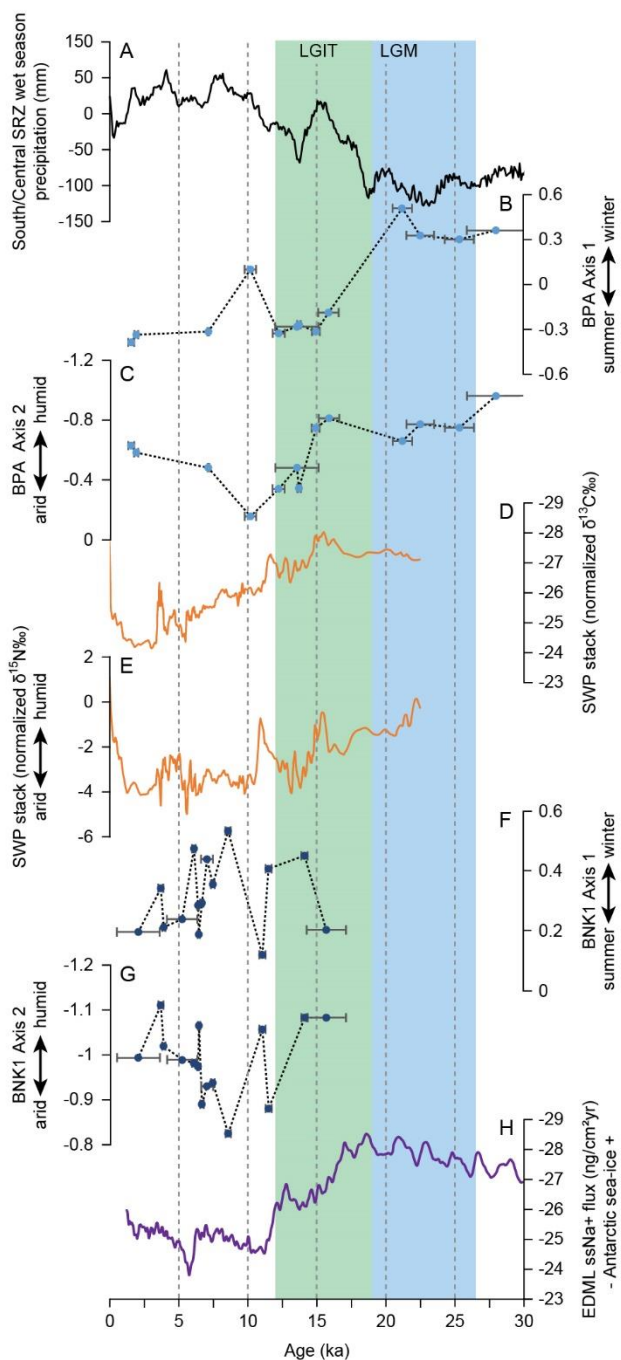
843 Cave and Byneskranskop 1 sequences.. Ages for CL3 and up represent calibrated 2σ

844 ranges of all ^{14}C ages in a given stratum, using SHCal13 (Hogg et al., 2013) calibration

845 data and OxCal 4.3 (Bronk Ramsey, 2009). Ages for GWA and below are modelled age

846 estimates from Pargeter et al. (2018).

847



848

849 **Figure 7.** Comparison of precipitation seasonality (axis 1) and aridity (axis 2)
 850 reconstructions from Boomplass Cave (BPA: B, C) and Byneskranskop 1 (BNK1: F, G)
 851 to local and regional proxy records, including (A) southern-central summer rainfall zone
 852 (SRZ) wet season precipitation (Chevalier and Chase, 2015), (D) $\delta^{13}\text{C}$ and (E) $\delta^{15}\text{N}$

853 stacks from the Seweweekspoort hyrax middens (Chase et al. 2017, 2018), and (H)
854 sea-salt sodium flux from the EDML ice core indicating Antarctic sea-ice extent (Fischer
855 et al. 2007). Undated fossil assemblages are not plotted here. Error bars for microfauna
856 assemblages correspond to age ranges reported in Figure 6.

857